catalysts

MDPI

Article

Selective Hydrogenolysis of Furfuryl Alcohol to Pentanediol over Pt Supported on MgO

Yuhao Yang, Qiaoyun Liu * and Zhongyi Liu *

College of Chemistry, Zhengzhou University, Zhengzhou 450066, China
* Correspondence: authors: liuqiaoyun@zzu.edu.cn (Q.L.); liuzhongyi@zzu.edu.cn (Z.L.)

Abstract: The catalytic conversion of naturally rich and renewable biomass into high-value chemicals is of great significance for pursuing a sustainable future and a green economy. The preparation of pentanediol from furfuryl alcohol is an important means of high-value conversion of biomass. The Pt-based catalyst supported on MgO was applied to the selective hydrogenation of biomass furfuryl alcohol to prepare pentanediol. By adjusting parameters such as catalyst loading, reduction temperature, reaction temperature, and pressure, a highly active catalyst was designed and the optimal catalytic hydrogenation conditions were determined. The hydrogenation experiment results showed that the selectivity of the 2Pt/MgO-200 catalyst for 1,2-pentanediol and 1,5-pentanediol reached 59.4% and 15.2%, respectively, under 160 °C and 1 MPa hydrogen pressure. The catalyst was characterized by X-ray powder diffraction (XRD), transmission electron microscopy (TEM), X-ray photoelectron spectrometer (XPS), CO_2-temperature programmed desorption (CO_2-TPD), and other methods. The characterization results indicate that the reduction temperature has a significant impact on the metal Pt, and an appropriate reduction temperature is beneficial for the hydrogenation performance of the catalyst. In addition, the basic sites on the carrier are also another important factor affecting the activity of the catalyst. In addition, stability tests were conducted on the catalyst, and the reasons for catalyst deactivation were studied using methods such as thermogravimetric analysis (TGA) and Fourier transform infrared spectroscopy (FT-IR). The results showed that the activity of the catalyst decreased after five cycles, and the deactivation was due to the hydrolysis of the carrier, the increase in metal particle size, and the surface adsorption of organic matter.

Keywords: selective hydrogenation; pentanediol; catalyst deactivation; basic site

Citation: Yang, Y.; Liu, Q.; Liu, Z. Selective Hydrogenolysis of Furfuryl Alcohol to Pentanediol over Pt Supported on MgO. *Catalysts* **2024**, *14*, 223. https://doi.org/10.3390/catal14040223

Academic Editors: Indra Neel Pulidindi, Aharon Gedanken, Pankaj Sharma and Ivan V. Kozhevnikov

Received: 24 January 2024
Revised: 29 February 2024
Accepted: 1 March 2024
Published: 27 March 2024

1. Introduction

With the decrease in oil resources together with the increase in demand for energy and political and environmental concerns about fossil fuels, research on the exploration of renewable resources for sustainable supply has been conducted [1,2]. Biomass, as the only renewable carbon source at present [3], can be effectively and cleanly converted into fuel and chemical products through chemical reactions and biological conversion [4].

The catalytic conversion of biomass and biomass-derived platform molecules into fuels and value-added chemicals has attracted widespread attention to the development of the sustainable chemical industry [5–7]. Furfuryl alcohol (FFA), as an important biomass derivative, has irreplaceable advantages in the green manufacturing of high value-added chemicals. Among them, pentanediol is one of the most valuable products derived from FFA hydrogenolysis, and it is widely used in industries such as the food, chemical, and pharmaceutical industries. 1,2-pentanediol (1,2-PeD) is a key raw material for synthesizing the fungicide propiconazole and is widely used as a pharmaceutical intermediate for synthesis. 1,5-pentanediol (1,5-PeD) is an important monomer for synthesizing polyester and polyurethane. In addition, it can also be used as antifreeze and green solvent for chemical synthesis [8].

In previous reports on the selective hydrogenation of furfural and its derivatives, Pt-based [9–11], Ru-based [12–14], Rh-based [15], Ni-based [16,17], Cu-based [18–20], and Pd-based [21,22] catalysts exhibited high activity. Götz et al. [23] prepared Ru/Al_2O_3 catalysts for waterborne hydrogenation of FFA. Under the conditions of 200 °C and 10 MPa H2 for 1 h, the yield of 1,2-PeD is 32%. Wang's team [10] pointed out that the Pt/CeO_2 catalyst can effectively catalyze the hydrogenation of FFA to 1,2-PeD. Extensive characterization indicates that the chemical state of Pt plays a crucial role in improving the catalytic activity and selectivity of 1,2-PeD, which is controlled by the surface oxygen vacancies of CeO_2 through metal carrier interactions. Zhu et al. [24] found that on the coordination unsaturated 3D Pt-Pt site, the hydrogenolysis of the furan ring occurs through the weakening and adsorption of furan C-O, resulting in 1,2-PeD as the main product. The dual functional Cu/MFI catalyst designed by Dai et al. [20] achieved selectivity of 1,5-PeD (69.2%) and 1,2-PeD (16.0%) at 160 °C and 2.5 MPa hydrogen pressure. Rizky Gilang Kurniawan et al. [25] designed a three-metal Ni-CoOx-Al_2O_3 mixed metal–metal oxide catalyst to efficiently convert FFA into 1,5-PeD in one pot with a high yield of 47.5% at 160 °C and an initial H_2 pressure of 3 MPa. In the past, some catalysts had many drawbacks, such as low activity and insufficient stability. Pt-based catalysts had advantages such as high activity for the hydrogenolysis of FFA. However, a satisfactory yield of pentanediol has not yet been obtained under mild conditions.

In this work, we prepared a series of catalysts through the equal volume impregnation method and screened the performance of Pt/MgO on the selective hydrogenolysis of FFA. On this basis, further comparative experiments were conducted to optimize the optimal reaction conditions and catalyst preparation method. After a series of characterizations, the effects of different preparation conditions on catalyst activity and the relationship between catalyst carrier alkalinity and catalytic performance were studied. In addition, the cyclic stability of the catalyst was further investigated and the reason for catalyst deactivation was explained through characterization methods such as thermogravimetry and inductively coupled plasma.

2. Results and Discussion

2.1. Discussion on FFA Hydrogenation Results

Figure 1 is a schematic diagram of some FFA hydrogenation product routes. FFA can be hydrogenated to form cyclopentanone, cyclopentanol, and THFA on the C=C double bond. The production of target products 1,2-PeD and 1,5-PeD involves the cleavage and hydrogenation of C-O bonds in the furan ring. It is reported that the hydrogenation of FFA to 1,2-PeD requires ring opening hydrogenation to produce the intermediate product 1-hydroxy 2-Pentanone [24], and then further hydrogenation of C=O double bond to obtain the target product. Therefore, it is necessary to design a catalyst that can efficiently open the ring and hydrogenation.

2.1.1. Catalyst Screening

Compared with other active metal catalysts such as Pd and Ru (Table 1), Pt-based catalysts show higher activity in the catalytic hydrogenation of FFA. Among them, the catalyst supported by MgO showed high selectivity in the hydrogenation of furfuryl alcohol to pentanediol in the aqueous phase. Therefore, Pt/MgO was selected for further exploration.

Pt/MgO was selected as the catalyst for the hydrogenation of furfuryl alcohol to pentanediol for further investigation. Further exploration of the effects of platinum loading and catalyst reduction temperature on hydrogenation performance was conducted. As shown in Figure 2a, under low loading (<1.5 wt%), the low amount of active metal leads to a lower conversion rate of furfuryl alcohol. When the loading amount increases to 2 wt%, the conversion rate of FFA and the selectivity of pentanediol was highest. Further increasing the loading of metal Pt resulted in a decrease in the selectivity of pentanediol with increased selectivity for THFA. This indicates that too high an amount of metal

would facilitate the hydrogenation of the C=C bond. Therefore, 2 wt% Pt/MgO is a more reasonable choice. Further investigation was conducted on the effect of reduction temperature on the hydrogenation performance of the catalyst. Figure 2b shows the hydrogenation performance of the catalyst at different reduction temperatures. Comparing the catalytic performance at reduction temperatures of 150, 200, 300, and 400 °C, it can be observed that the conversion rate of FFA increases first and then decreases with increasing temperature. When the reduction temperature is 200 °C, the catalyst activity is optimal. After 6 h of reaction, the conversion rate of FFA reached 63.9%, and the selectivity of 1,2-PeD and 1,5-PeD were 58.2% and 12.7%, respectively. Therefore, 2 wt% Pt/MgO-200 was chosen as the catalyst for FFA hydrogenation and further exploration was conducted.

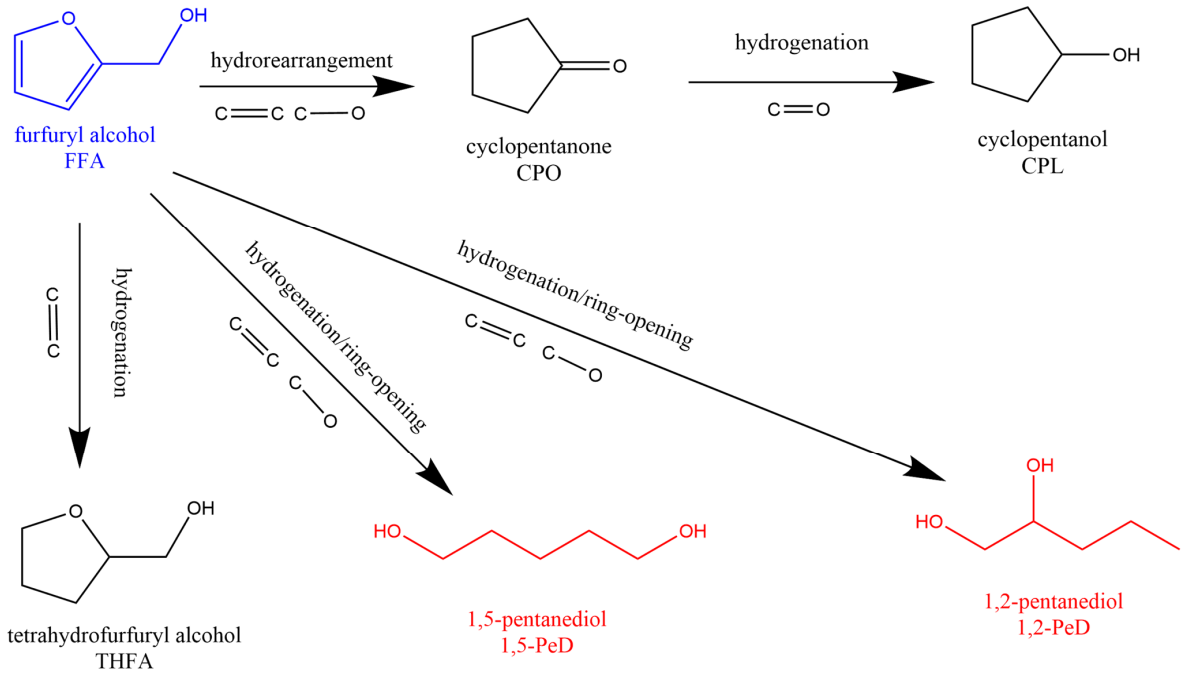

Figure 1. The reaction network of furfuryl alcohol hydrogenation and reaction path.

Table 1. Catalytic performance of different catalysts on the hydrogenolysis of FFA.

Entry	Catalysts	Conversion (%)	Selectivity (%)						
			1,2-PeD	1,5-PeD	1-Pentanol	CPO	CPL	THFA	Others
1	Pt/CeO_2	99.9	18.5	5.1	1.4	26.3	39.1	9.5	0.1
2	Pt/Fe_2O_3	99.9	1.5	/	/	53.3	45.2	/	/
3	Pt/TiO_2	99.9	34.8	3.6	7.9	47.7	1.5	3.3	1.2
4	Pt/ZrO_2	99.9	1.1	/	/	84.4	7.5	1.3	5.7
5	$Pt/a\text{-}Al_2O_3$	92.3	41.1	11.1	4.4	23.6	3.5	16.3	/
6	$Pt/\gamma\text{-}Al_2O_3$	87.3	37.7	15.1	2.6	10.8	/	31.6	2.2
7	Pt/MgO	96.8	58.4	12.8	1.7	1.3	0.5	17.9	7.4
8	Pd/MgO	93.5	3.7	1.1	/	2	/	89.8	3.4
9	Ru/MgO	15.8	13.2	/	/	17.7	/	47.5	21.6
10	Cu/MgO	16.8	33.9	8.9	/	35.1	/	21.4	0.7
11	Fe/MgO	7.5	17.3	/	/	34.7	/	20	28
12	Ni/MgO	6.3	/	/	/	38.1	/	23.8	38.1

Reaction conditions: 1.1 g FFA, 28.9 g H_2O, 0.2 g catalyst, 160 °C, 1 MPa H_2, 8 h. The metal loading mass in the catalyst is 2%.

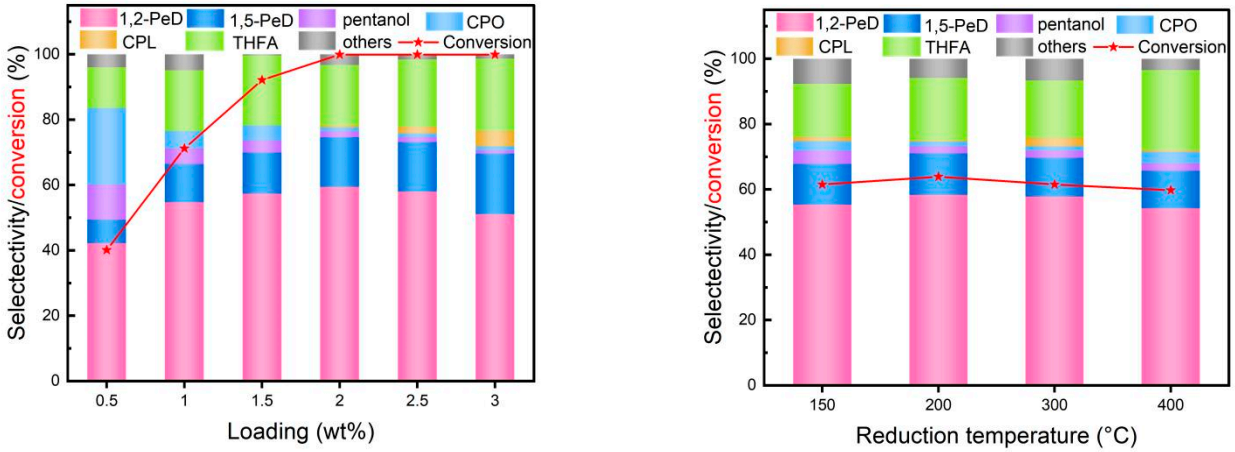

Figure 2. Catalytic conversion of FFA over Pt/MgO at (**a**) different metal loading and (**b**) different reduction temperatures. Reaction conditions: 1.1 g FFA, 28.9 g H_2O, 0.2 g catalyst, 160 °C, 1 MPa H_2, (**a**) 10 h and (**b**) 6 h.

To investigate the effect of reduction time on catalyst activity, the reduction temperature was controlled at 200 °C, and performance analysis was conducted on catalysts with different reduction times. As shown in Figure 3, when the reduction time is 0.5 h, the conversion rate of furfuryl alcohol is 75.8%, and the selectivity of the main byproduct tetrahydrofurfuryl alcohol reaches 37.2%, while the selectivity of the target product 1,2-PeD is only 45.7%. Extending the reduction time to 1 h, the conversion rate of furfuryl alcohol exceeded 99%, and the selectivity of 1,2-PeD reached 59.4%. Subsequently, by further prolonging the reaction time, there was no significant change in the catalyst activity. Therefore, it is believed that a time of 1 h is sufficient for the reduction of the catalyst.

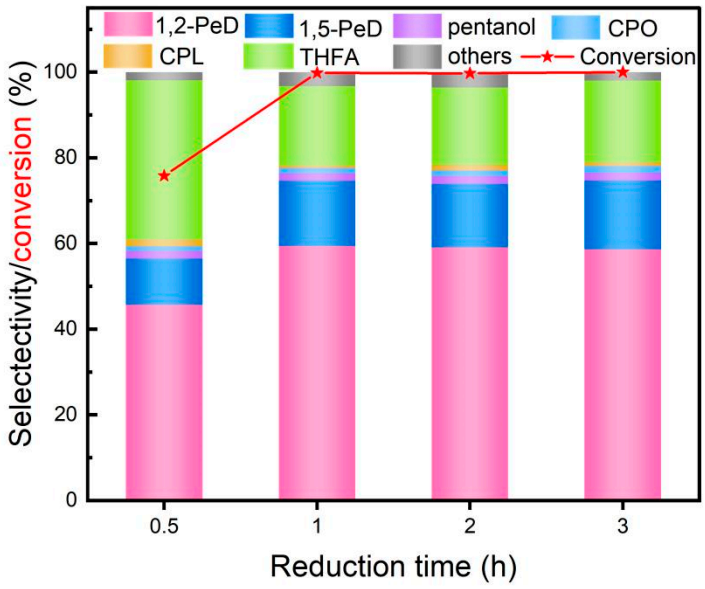

Figure 3. Catalytic conversion of FFA on Pt/MgO under reduction time. Reaction conditions: 1.1 g FFA, 28.9 g H_2O, 0.2 g catalyst, 160 °C, 1 Mpa H_2, 10 h.

2.1.2. Optimization of Catalytic Conditions

Reaction temperature is one of the key factors in chemical reactions, affecting the reaction rate and product selectivity. In order to explore the effect of reaction temperature on FFA hydrogenation, research was carried out within the range of 120 °C~200 °C. As

shown in Figure 4a, when the reaction temperature is controlled at 120 °C, the conversion rate of FFA after 6 h of reaction is about 40%. By further increasing the reaction temperature, the FFA conversion rate gradually increases. Meanwhile, it is found that in the temperature range of 120~200 °C, low temperature (<140 °C) is favorable for hydrogenation to THFA, while high temperature (>180 °C) conditions are more prone to rearrangement reactions to generate CPO, etc. At 160 °C, the comprehensive selectivity of pentanediol reaches its highest, with the selectivity of 58.3% and 12.7% for 1,2-PeD and 1,5-PeD, respectively.

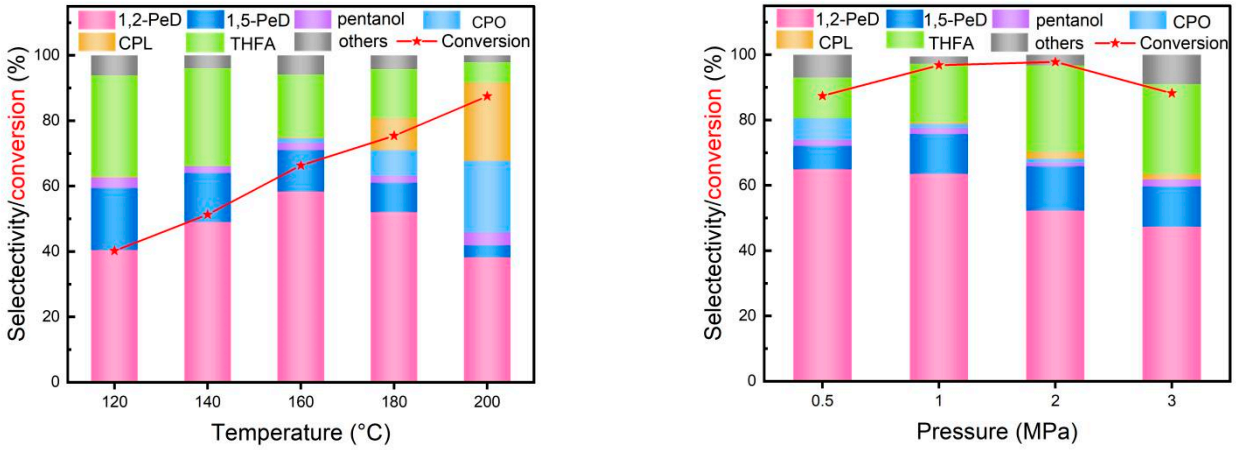

Figure 4. Catalytic conversion of FFA over 2Pt/MgO-200 at different (**a**) temperatures and (**b**) pressures. Reaction conditions: 1.1 g FFA, 28.9 g H_2O, 0.2 g catalyst. (**a**) 1 MPa H_2, 6 h; (**b**) 160 °C, 8 h.

Then, the temperature of the hydrogenation reaction was controlled at 160 °C and different hydrogen pressures were adjusted to explore the effect of reaction pressure on FFA hydrogenation. During this process, we appropriately shortened the reaction time to 8 h to demonstrate the effect of pressure on the selectivity of the target product. Figure 4b shows the hydrogenation results of hydrogen pressure within the range of 0.5~3 Mpa. It was found that at low hydrogen pressure, the reaction rate is slow and the conversion of furfuryl alcohol is not high. After increasing the pressure, the conversion rate significantly increases. However, a decrease in the selectivity of pentanediol was observed when the pressure increased. Therefore, 1 Mpa was chosen as the appropriate hydrogen reaction pressure.

In industrial production, controlling the amount of catalyst is crucial for reducing production costs. We investigated the effect of different 2Pt/MgO-200 catalyst dosages on the hydrogenation reaction and found that within a certain range (Figure 5), the conversion rate of furfural alcohol showed an upward trend with the increase in catalyst dosages. When the catalyst dosages increased to 0.2 g, the conversion rate of FFA reached the highest, and at this time, the comprehensive selectivity of pentanediol also reached its peak. When continuing to increase the catalyst input, the conversion rate of FFA and the selectivity of pentanediol did not increase. The concentration of the substrate also affects the yield of the product. Examining the hydrogenation reaction of FFA at different concentrations, it was found that at a higher concentration, the conversion rate of FFA significantly decreased, and the selectivity of 1,2-PeD also decreased to some extent (Figure 5b). Therefore, 0.2 g catalyst was selected to be added at a substrate concentration of 0.35 mol/L for further exploration.

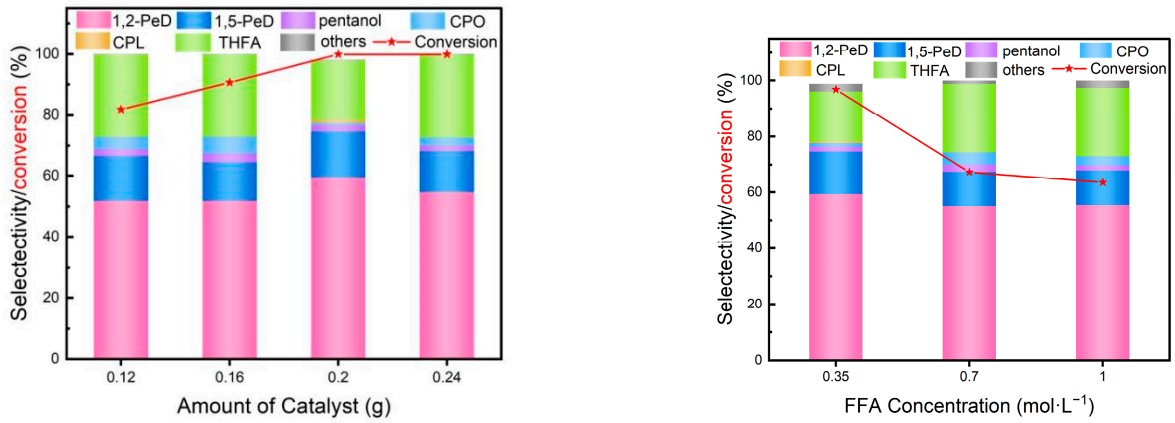

(**a**) (**b**)

Figure 5. The influence of (**a**) catalyst amount and (**b**) substrate concentration on hydrogenation results. Reaction conditions: (**a**) 1.1 g FFA, 28.9 g H_2O; (**b**) 0.2 g catalyst, 160 °C, 1 MPa H_2, 10 h.

In order to elucidate the changes of product distribution during the hydrogenation reaction process, a curve was drawn for the relationship between yield and time. Figure 6a shows the changes of various substances in the system at different times. It can be seen that during the hydrogenation of furfuryl alcohol, the yield of 1,2-PeD increases the fastest, followed by 1,5-PeD and THFA. In addition, due to the influence of the substrate concentration, the conversion rate of the reaction in the first eight hours is significantly higher than that in the next two hours. In addition, the hydrogenation performance of Pt-based catalysts for furfuryl alcohol under different solvents was investigated. Previous literature has shown that in the hydrogenation of furfuryl alcohol catalyzed by active metal Pt, water plays a decisive role in the ring opening process of furfuryl alcohol and can improve the selectivity of 1,2-PeD [26]. As shown in Figure 6b, the yield of 1,2-PeD in the hydrogenation of furfuryl alcohol in organic solvents ethanol and isopropanol is much lower than in water, which is consistent with previous conclusions.

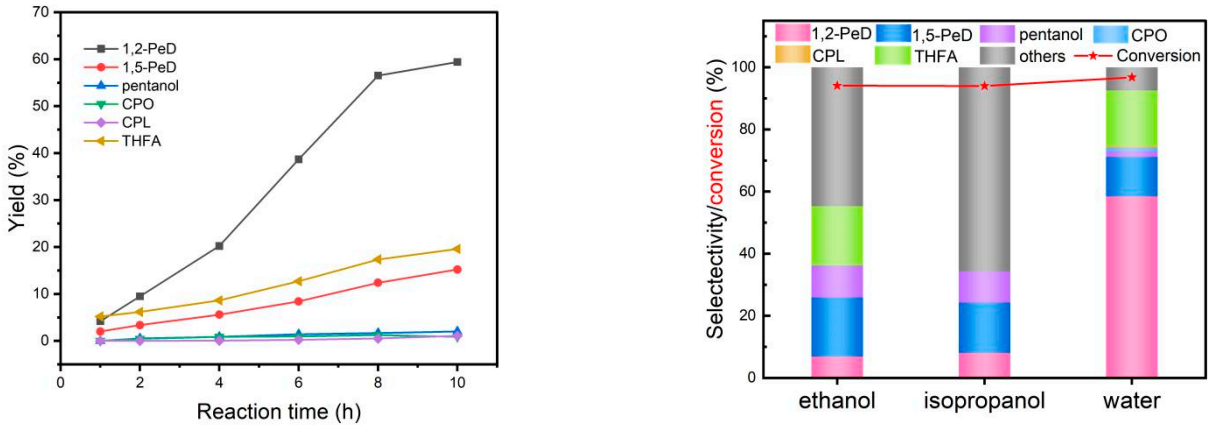

(**a**) (**b**)

Figure 6. FFA conversion and product selectivity over 2Pt/MgO-200. Reaction conditions: (**a**) 1.1 g FFA, 28.9 g H_2O, 0.2 g catalyst, 160 °C, 1 MPa H_2; (**b**) 1.1 g FFA, 28.9 g H_2O, 0.2 g catalyst, 160 °C, 1 MPa H_2, 8 h.

2.2. Characterization Results

2.2.1. XRD Result Analysis

The formation of crystalline species in different catalysts was studied using wide-angle XRD technology, as shown in Figure 7. The results show that all peaks are related to the

carrier [27] (2θ = 37, 43, 62, 75, 78 °), and no diffraction peaks of metal Pt were observed during reduction within the temperature range of 150–400 °C. This indicates the low loading of metal or the generation of small-sized and highly dispersed metal nanoparticles during the reduction process.

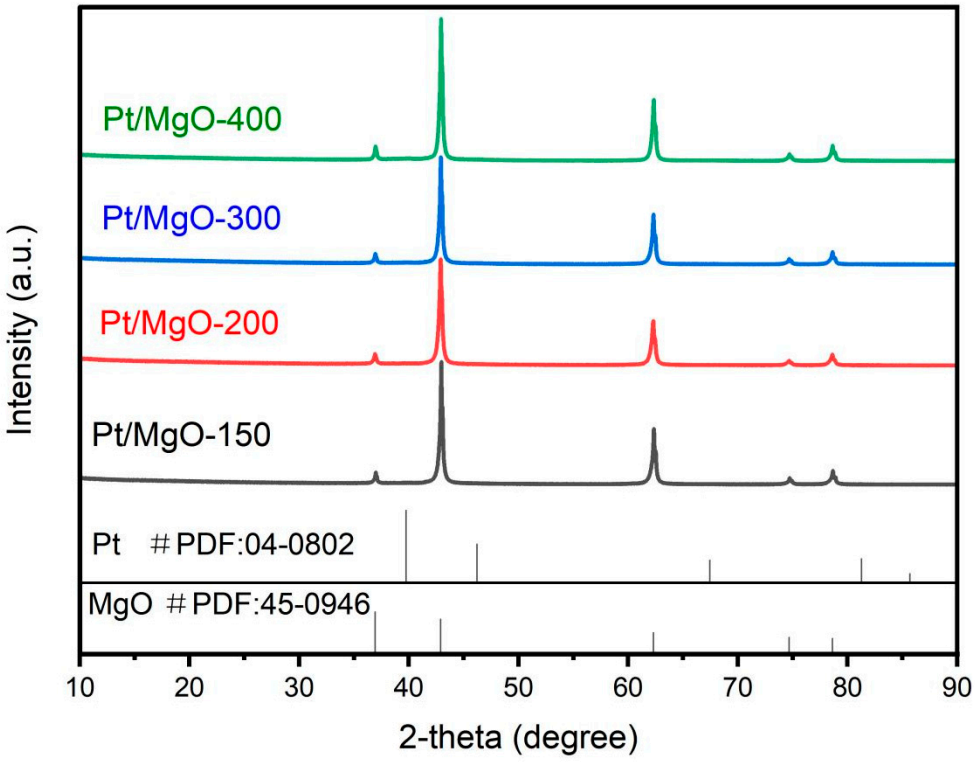

Figure 7. XRD patterns of 2Pt/MgO at different reduction temperatures.

2.2.2. TEM

From the hydrogenation performance Figure 2b, it can be observed that the reduction temperature has a significant impact on the activity of the catalyst. According to Figure 8, when the catalyst reduction temperature is not higher than 200 °C, the average particle size of metal Pt is about 1.62 nm. Further increasing the reduction temperature to 300 °C and 400 °C, the average particle size of Pt metal is 2.38 nm and 2.40 nm, respectively. Overall, higher temperatures lead to larger active metal particles in the catalyst, which is not favorable for the cleavage of the C-O bond, and it is more prone to the hydrogenation of the C=C bond, thus leading to the decreased selectivity of pentanediol.

2.2.3. H_2-TPR

In order to further explore the interaction between active metals and carriers, the catalyst samples were characterized by temperature programmed reduction. Figure 9 shows the H_2-TPR curve of Pt-based catalysts. It can be clearly observed that the Pt/MgO catalyst has a sharp main peak at 160 °C and a small peak near 350 °C, respectively. The small peak at 350 °C might be caused by the aggregation of metal nanoparticles. From H_2-TPR, Pt nanoparticles can be mostly reduced before 250 °C.

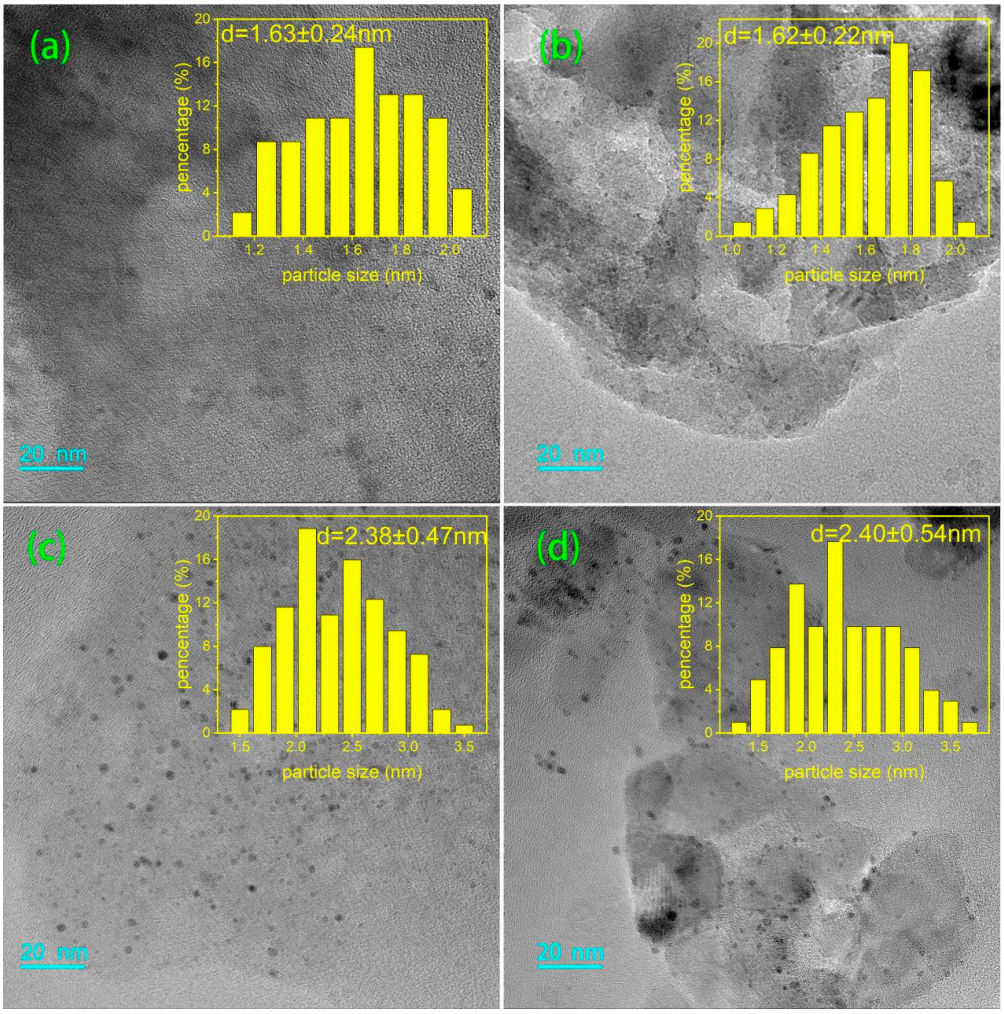

Figure 8. HRTEM images and particle size distribution of (**a**) Pt/MgO-150, (**b**) Pt/MgO-200, (**c**) Pt/MgO-300, (**d**) Pt/MgO-400.

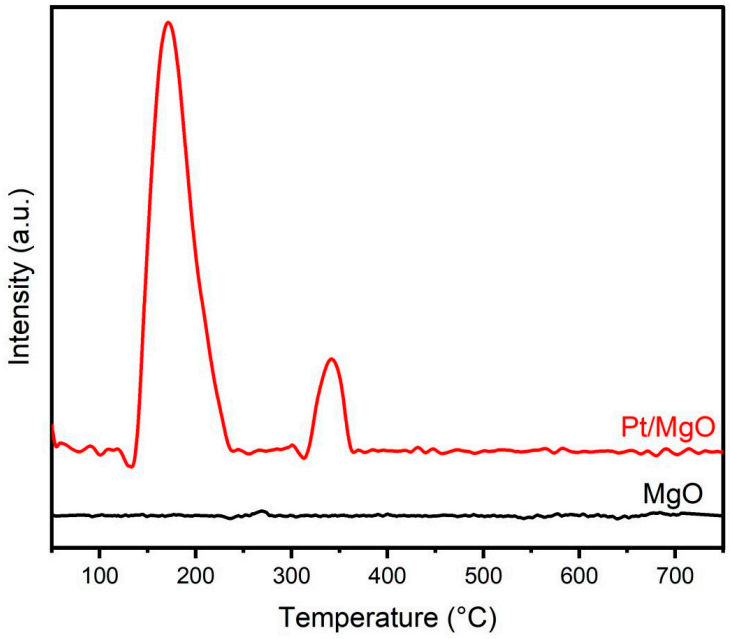

Figure 9. H_2-TPR spectra of Pt/MgO and MgO.

2.2.4. XPS Analysis

In the XPS spectrum, as shown in Figure 10, the Pt 4f spectrum of the Pt/MgO catalyst can be deconvoluted into three Pt species, with Pt 4f 7/2 Bes at 71.0 (Pt^0), 72.4 (Pt^{2+}), and 74.9 eV (Pt^{4+}) [28], respectively. It can be observed from the table that the relative ratios for 2Pt/MgO-200 of Pt^0, Pt^{2+}, and Pt^{4+} species are 34%, 37%, and 28%, respectively. Comparing the XPS spectra (Figure 10a) and elemental valence analysis (Table 2) under different temperature reduction conditions, it was found that the proportion of Pt^0 in the catalyst after low-temperature reduction (150 °C) was only 26%, and the main forms of metal Pt in the catalyst were Pt^{2+} and Pt^{4+}. After further increasing the reduction temperature, it was found that more active metal Pt was reduced in the catalyst. After reduction at 400 °C, the proportion of Pt^0 reached 50%, which is consistent with the results of H_2-TPR.

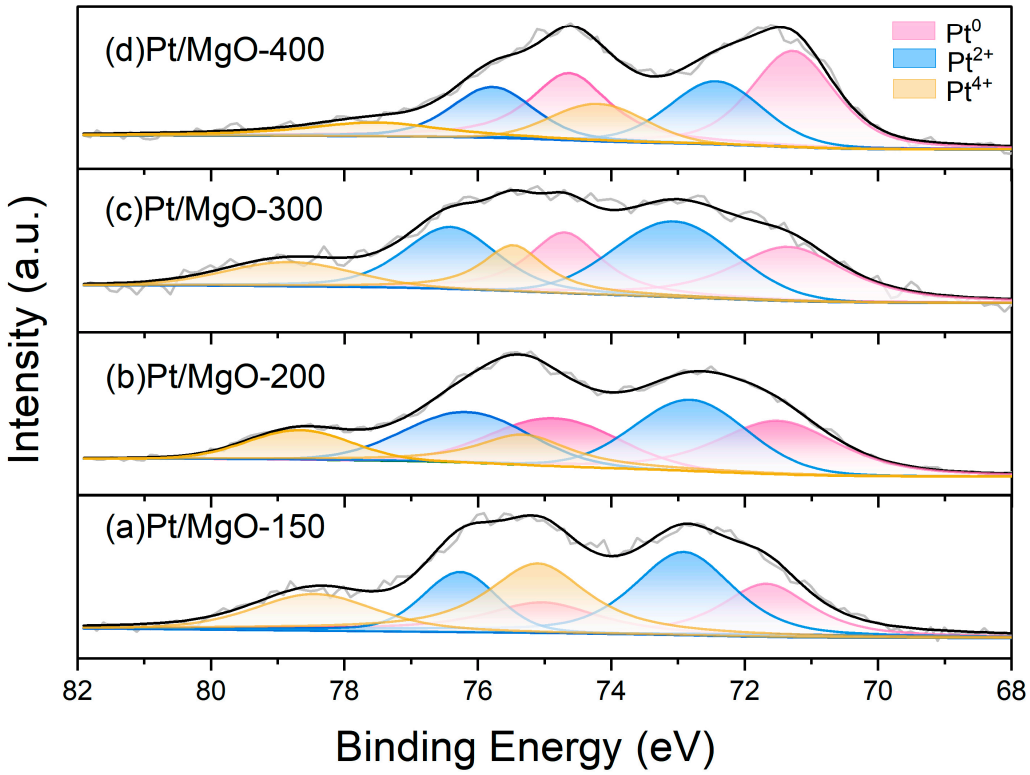

Figure 10. XPS spectra of Pt/MgO at different reduction temperatures.

Table 2. XPS analysis of Pt/MgO at different reduction temperatures.

Catalysts	$Pt^0{}_{7/2}$		$Pt^{2+}{}_{7/2}$		$Pt^{4+}{}_{7/2}$	
	B.E. (eV)	Ratio (%)	B.E. (eV)	Ratio (%)	B.E. (eV)	Ratio (%)
Pt/MgO-150	71.6	26	72.9	39	75.1	35
Pt/MgO-200	71.5	34	72.8	37	75.3	28
Pt/MgO-300	71.2	38	73.0	42	75.4	19
Pt/MgO-400	71.3	50	72.4	32	74.2	18

Based on the results of hydrogenation (Figure 2b), TEM and XPS analysis indicate that metal Pt cannot be fully reduced at lower reduction temperatures. Raising the reduction temperature promotes the reduction of metal Pt, but at high temperatures, the particle size of Pt nanoparticles significantly increases, the metal dispersion decreases, and the catalytic activity decreases. Therefore, comprehensive consideration suggests that reduction at 200 °C is the optimal reduction temperature.

2.2.5. CO_2-TPD

According to previous reports [29,30], the basic sites on the catalyst play an important role in the ring-opening of furan rings in furfuryl alcohol. Through the CO_2-TPD spectrum (Figure 11), we found that the carrier MgO exhibited moderate intensity of basic sites at 300–350 °C, and the basic sites were not destroyed during the preparation process of 2Pt/MgO-200. As a comparison, almost no basic sites were observed in the CO_2-TPD spectrum of Pt/TiO_2, indicating that its alkalinity is much lower than that of 2Pt/MgO-200. And the total selectivity of Pt/TiO_2 for pentanediol in furfuryl alcohol hydrogenation is only 38.4%, with higher selectivity for CPO, which indicates that the rearrangement of the furan ring would compete with the hydrogenolysis of the C-O bond under the reaction conditions (Table 1, entry 3). This indicates that the selective hydrogenolysis of FFA is favorable under the basic sites.

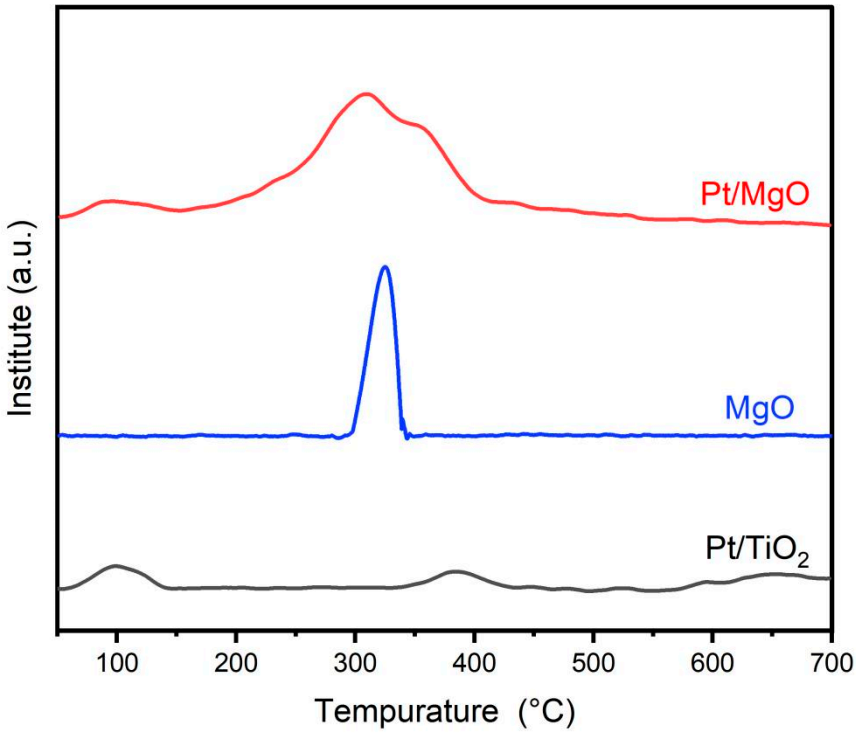

Figure 11. CO_2-TPD spectra of 2Pt/MgO-200 and 2Pt/TiO_2-200.

2.3. Exploring the Stability and Deactivation Causes of Catalysts

2.3.1. Catalyst Cycle Stability

In order to verify the cyclic stability of the catalyst, the cyclic performance of 2Pt/MgO-200 was tested under optimized reaction conditions. The experimental results are shown in Figure 12, and the performance of the 2Pt/MgO-200 catalyst maintained high activity in the first four cycles. In the fifth cycle, the conversion and selectivity for pentanediol decreased to 93.8% and 65.3%, respectively.

2.3.2. Exploring the Causes of Catalyst Deactivation

It is generally believed that in the process of heterogeneous catalysis, the causes of catalyst deactivation include toxic adsorption, the loss of active metals, and the enlargement of metal nanoparticles [31,32]. To investigate the reasons for catalyst deactivation during the hydrogenation of FFA, 2Pt/MgO-200 catalysts before and after cyclic testing were characterized by thermogravimetry and electron microscopy.

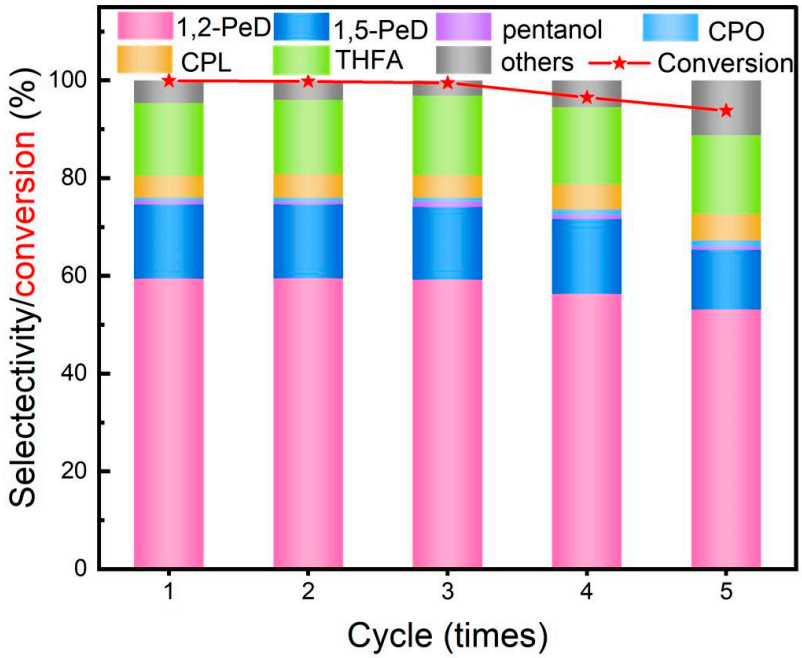

Figure 12. Cycling tests of FFA over the 2Pt/MgO-200 catalyst. Reaction conditions: 1.1 g FFA, 28.9 g H_2O, 0.2 g catalyst, 160 °C, 1 MPa H_2, 10 h. Catalysts were reused after centrifugation and drying.

Considering the instability of MgO carrier in water, XRD characterization was performed on the catalyst before and after cycling. As shown in Figure 13, it can be observed on the XRD spectrum of the catalyst after cycling. The diffraction peaks at 18.5, 32.8, 37.9, 50.8, 58.6, 62.1, 68.2, 72.1, and 81.3° correspond to the crystal planes of $Mg(OH)_2$ at 001, 100, 101, 102, 110, 111, 103, 201, and 202, respectively. The diffraction peak at 42.9° belongs to the 200 crystal plane of MgO. This indicates that the catalyst carrier MgO after the reaction is hydrolyzed into $Mg(OH)_2$, and during the catalytic process, the carrier may exist in the form of a complex of oxides and hydroxides. In addition, the diffraction peaks at the diffraction angles of 39.7° and 46.2° belong to the 111 and 200 crystal planes of the metal Pt. This indicates that there may be aggregation of active metal Pt on the catalyst after cycling.

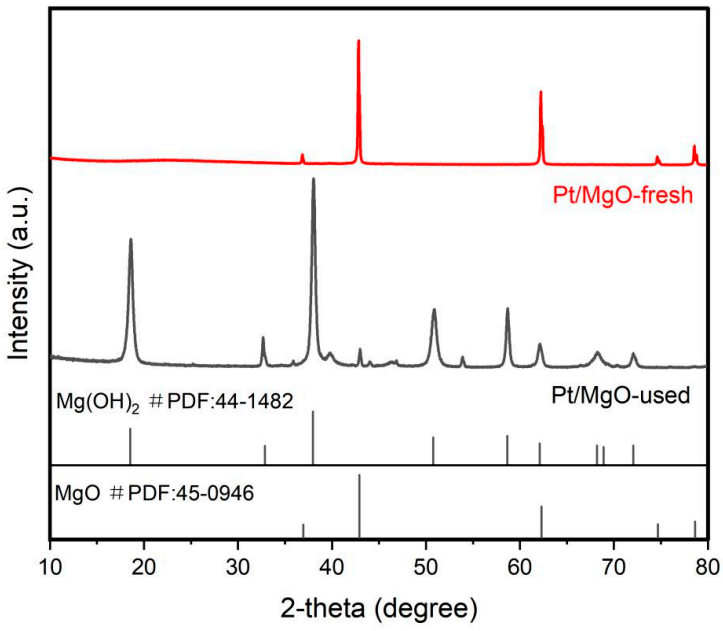

Figure 13. XRD patterns of 2Pt/MgO-200 before and after cycling.

Figure 14 shows the thermogravimetric curves of fresh and used 2Pt/MgO-200. It can be seen that at the high temperature of 800 °C, the mass of the unused catalyst only decreased to 96% even though treated until 800 °C, which might be caused by the adsorbed water in the catalyst. However, for the used 2Pt/MgO-200 after five cycling tests, the mass decreased obviously at 300 °C and further decreased to 65% after 550 °C. The mass decrease of the 2Pt/MgO-200 used might be ascribed to the organic matter adsorbed on the catalyst surface.

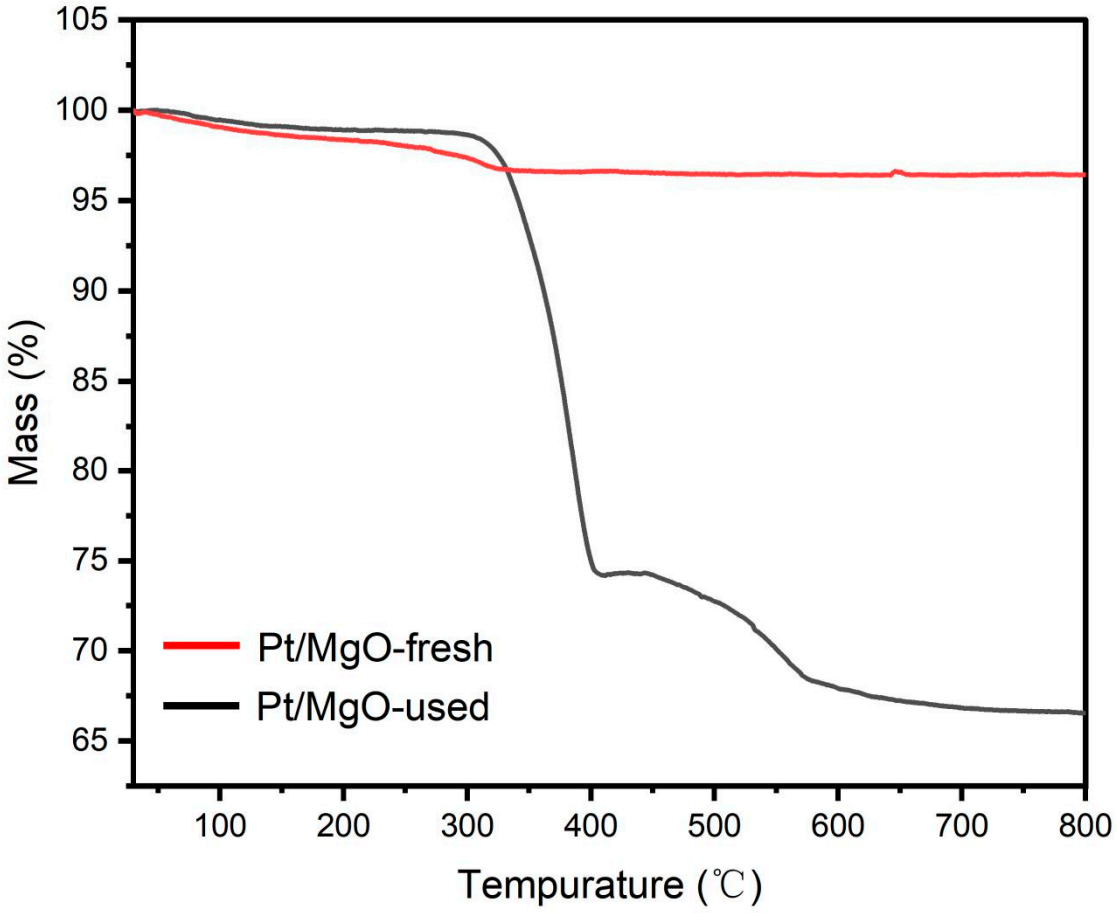

Figure 14. Thermogravimetric spectra of fresh and used 2Pt/MgO-200.

To further illustrate the adsorption of organic compounds on the catalyst, infrared spectroscopy characterization was performed on the catalyst before and after use. As shown in Figure 15, the absorption peaks at 2967 cm^{-1} and 2877 cm^{-1} are attributed to the stretching vibration of the methyl group. The absorption peaks at 1594 cm^{-1} and 1504 cm^{-1} are attributed to the stretching vibration of C=C on the furan ring. The absorption peaks at 1221 cm^{-1}, 1149 cm^{-1}, and 1074 cm^{-1} correspond to the stretching vibrations of C-C, C-O-C, and C-O on the furan ring, respectively [24]. As a comparison, no infrared absorption peak was observed on the fresh catalyst. Based on this, it is believed that there is adsorption of organic compounds such as furfuryl alcohol on the catalyst after cycling.

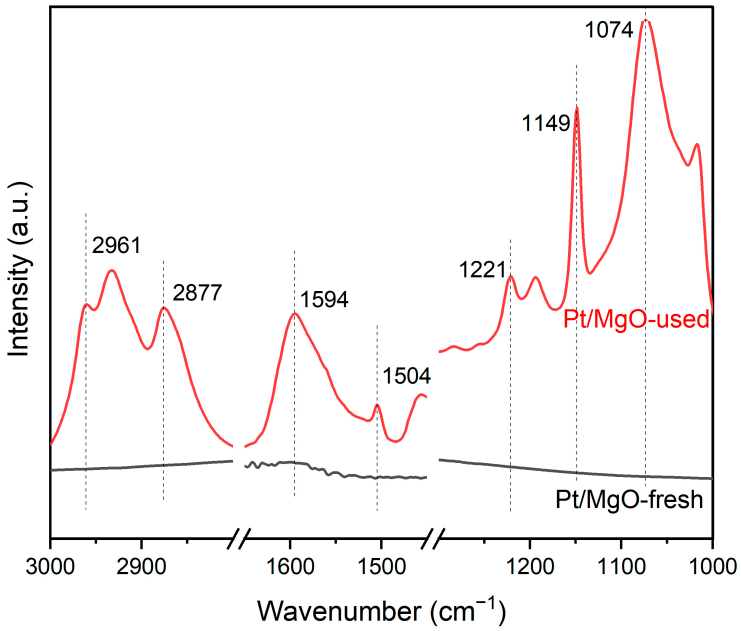

Figure 15. FT-IR spectra of Pt/MgO before and after cycling.

Figure 16 shows the particle size analysis of the catalyst before and after the 2Pt/MgO-200 cycles. The size of metal Pt particles in the catalyst increased from 1.62 nm to 2.59 nm after five cycles of testing. The increase in particle size will lead to a decrease in metal dispersion, which is another important reason for the decrease in catalyst activity.

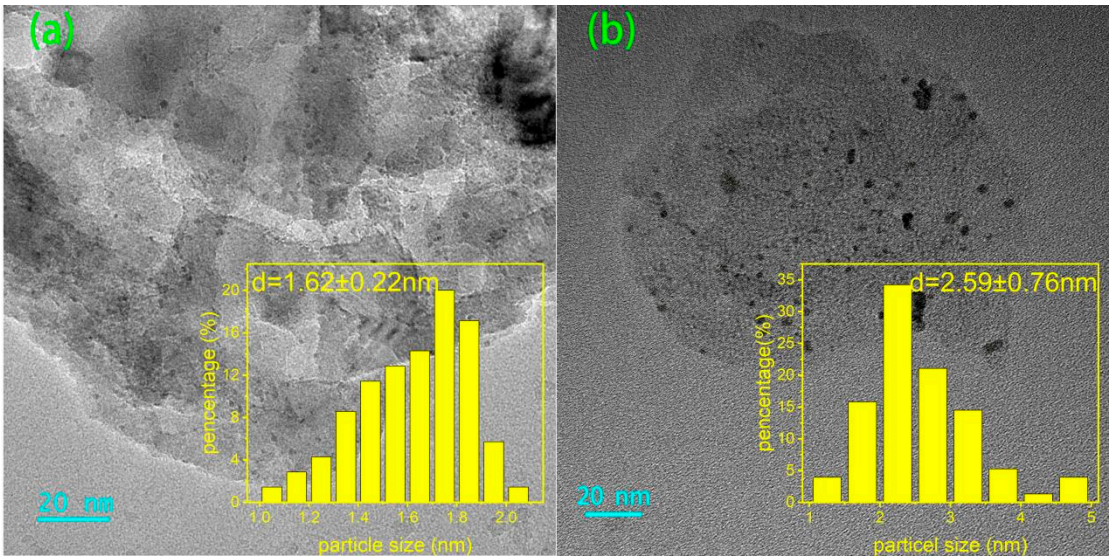

Figure 16. TEM images and particle size distribution of 2Pt/MgO-200 (**a**) fresh and (**b**) recycled.

In summary, the deactivation of the catalyst is due to the hydrolysis of the carrier, the adsorption of organic matter, and the growth of the active metal particle size.

3. Experimental Section

3.1. Catalyst Preparation

Materials: $H_2PtCl_6{\cdot}6H_2O$ (Aladdin, Vienna, Virginia, USA), $Co(NO_3)_2{\cdot}6H_2O$, $Fe(NO_3)_3{\cdot}9H_2O$, $NiC_4H_6O_4{\cdot}4H_2O$ (99.9%), $(CH_3COO)_2Mn$ (Aladdin, 99%), $Cu(NO_3)_2{\cdot}3H_2O$, $ZnSO_4{\cdot}7H_2O$ (92%), MgO(Aladdin, AR), CeO_2 (Aladdin, 99%), $RuCl_3$ (97%), $PdCl_2$ (Aladdin, 99%), Active carbon (Aladdin, AR), TiO_2 (Aladdin, 99%), and Al_2O_3 (Aladdin, 99%).

The catalyst was prepared using an equal volume impregnation method. In a typical preparation, a certain amount of chloroplatinic acid aqueous solution was accurately added to a certain mass of MgO powder and stirred for 20 min. Then the mixture was kept stewing at room temperature for 6–8 h and then dried overnight at 60 °C. Next, the powder was calcinated under air at 350 °C for 3 h. Finally, the catalyst was reduced under H_2 atmosphere at different temperatures for 1 h. The final catalyst is expressed as xPt/MgO-T, where x represents the mass loading of Pt and T represents the reduction temperature.

3.2. Catalyst Characterization

X-ray diffraction (XRD) measurements were performed on an X'Pert PRO diffractometer using Cu Kα radiation (λ = 0.154 nm) operated at 40 kV and 45 mA. The patterns were recorded from 10 to 90° in 2θ with a scan speed of 10° min^{-1}.

The transmission electron microscopy (TEM) tests were carried out on JEM 2800 instruments of JEOL Company in Japan (Tokyo, Japan) with a working voltage of 200 KV.

The X-ray photoelectron spectroscopy was obtained using the PHI Quantera SXM spectrometer, and the laboratory used Al targets with Kα = 1486.6 eV as the radiation source. When estimating the binding energy (BE) values of various elements, the peak corresponding to C 1s (284.8 eV) was taken as a reference.

Infrared testing was performed on a Nicolet 6700 Fourier transform infrared spectrometer equipped with an MCT detector. Approximately 150 mg of catalyst sample was weighed and pressed into KBr tablets, then placed in a sample cell for testing.

The chemical adsorption was tested on Micromeritics Auto Chem 2910. Hydrogen Temperature Programmed Reduction (H_2-TPR) was used to determine the reduction properties of metal sites in the analytical catalysts. A total of 0.15 g unreduced catalyst was placed in a quartz tube and treated with Ar (99.999%, 30 mL/min) at 200 °C for 1 h to remove adsorbed water and other impurities. Then, a gas mixture of H_2 (10%)-Ar (90%) was passed through the U-shaped tube at 50 °C, and the temperature was raised to 800 °C at a heating rate of 10 °C/min. The rate of H_2 consumption was monitored by a thermal conductivity detector (TCD). Carbon Dioxide Temperature Programmed Desorption (CO_2-TPD) was used to test the basic sites. In a typical experiment, 0.15 g of catalyst sample was placed in a U-shaped flow through a quartz sample tube. Before measurement, the reduced catalyst was pretreated in Ar (99.999%, 30 mL/min) at 200 °C for 1 h. A mixture of CO_2 was injected in Ar (10%) at 30 °C (30 mL/min) for 30 min. Then, the sample was treated with Ar (30 mL/min) at 30 °C for 1 h. Finally, the temperature was increased from room temperature to 700 °C in an Ar atmosphere and the TCD signals were continuously collected.

3.3. Catalytic Performance Evaluation

Selective hydrogenolysis of FFA was carried out at a speed of 600 r/min in a 100 mL high-pressure reactor. All calcined samples were used in powder form. In a typical operation, 30 g of 4 wt% FFA aqueous solution and a certain amount of the reduced catalyst were introduced into the reactor. After blowing with H_2 at least three times, the reactor was pressurized to 1 MPa and heated to 160 °C to begin the reaction.

After the reaction, the products were centrifuged and the supernatant was identified using Agilent GC-7800A gas chromatography (Santa Clara, California, United States) and Pfeiffer Omnistar GSD 320 mass spectrometer (GC-MS). The conversion rate and product selectivity were determined using the external standard method, and the calculation formula is as follows:

$$\text{FFA Conversion (\%)} = [(\text{FFA}_{\text{before}} - \text{FFA}_{\text{after}})/\text{FFA}_{\text{before}}] \times 100\%$$

$$\text{Product Selectivity (\%)} = [\text{Product}_{\text{after}}/(\text{FFA}_{\text{before}} - \text{FFA}_{\text{after}})] \times 100\%$$

3.4. Cycling Test

The cycling experiment involves recycling the catalyst after reactions. After each reaction, all products in the reactor were centrifuged and the catalyst powder was collected. The collected catalyst was washed with deionized water and then centrifuged. Finally, it was dried in a vacuum oven, ground, and subjected to the next hydrogenation reaction.

4. Conclusions

In the experiment of the catalytic hydrogenation of furfuryl alcohol to pentanediol, Pt/MgO showed good catalytic activity. Two percent Pt/MgO reduced at 200 °C showed the optimal catalytic performance. At 160 °C and 1 MPa H_2 pressure, when the concentration of furfuryl alcohol was 0.35 mol/L and 0.2 g of catalyst was added, the FFA conversion rate reached 100% within 10 h. The selectivity of 1,2-PeD and 1,5-PeD was 59.4% and 15.2%, respectively, with the total yield of pentanediol reaching 74.6%. Detailed characterization indicates that the reduction temperature has a significant impact on the chemical state of Pt and the particle size distribution. A low reduction temperature led to the insufficient reduction of metal Pt, which is unfavorable for the cleavage of the C-O bond. And a high reduction temperature would cause the aggregation of Pt nanoparticles, which would lead to low metal utilization and the hydrogenation of the C=C bond, thus decreasing the conversion and selectivity for pentanediol. In summary, the highly dispersed metallic Pt nanoparticles facilitate the selective hydrogenolysis of FFA to pentanediol. In addition, the basic sites on the MgO carrier are also the key to the ring-opening hydrogenation of FFA. The deactivation of catalysts during hydrogenation is caused by the hydrolysis of the support, adsorption of organic chemicals, and growth in the size of loaded metal particles. This work provides a meaningful reference for the hydrogenation of FFA to prepare pentanediol.

Author Contributions: Conceptualization, Q.L. and Y.Y.; methodology, Q.L.; validation, Y.Y.; formal analysis, Y.Y.; investigation, Y.Y.; resources, Z.L.; data curation, Q.L.; writing—original draft preparation, Y.Y.; writing—review and editing, Q.L.; visualization, Y.Y.; supervision, Q.L.; project administration, Z.L.; funding acquisition, Z.L. All authors have read and agreed to the published version of the manuscript.

Funding: This work was financially supported by the National Natural Science Foundation of China (22278380) and the China Postdoctoral Science Foundation (2021M692911).

Data Availability Statement: The data that support the findings of this study are available from the corresponding authors upon reasonable request.

Conflicts of Interest: The authors declare no conflicts of interest.

References

1. Mika, L.T.; Csefalvay, E.; Nemeth, A. Catalytic Conversion of Carbohydrates to Initial Platform Chemicals: Chemistry and Sustainability. *Chem. Rev.* **2018**, *118*, 505–613. [CrossRef]
2. Chheda, J.N.; Huber, G.W.; Dumesic, J.A. Liquid-phase catalytic processing of biomass-derived oxygenated hydrocarbons to fuels and chemicals. *Angew. Chem. Int. Ed. Engl.* **2007**, *46*, 7164–7183. [CrossRef]
3. Nigam, P.S.; Singh, A. Production of liquid biofuels from renewable resources. *Prog. Energy Combust. Sci.* **2011**, *37*, 52–68. [CrossRef]
4. Srivastava, R.K. Bio-energy production by contribution of effective and suitable microbial system. *Mater. Sci. Energy Technol.* **2019**, *2*, 308–318. [CrossRef]
5. Serrano-Ruiz, J.C.; Luque, R.; Sepulveda-Escribano, A. Transformations of biomass-derived platform molecules: From high added-value chemicals to fuels via aqueous-phase processing. *Chem. Soc. Rev.* **2011**, *40*, 5266–5281. [CrossRef]
6. Li, C.; Zhao, X.; Wang, A.; Huber, G.W.; Zhang, T. Catalytic Transformation of Lignin for the Production of Chemicals and Fuels. *Chem. Rev.* **2015**, *115*, 11559–11624. [CrossRef]
7. Zhang, Z.; Song, J.; Han, B. Catalytic Transformation of Lignocellulose into Chemicals and Fuel Products in Ionic Liquids. *Chem. Rev.* **2017**, *117*, 6834–6880. [CrossRef] [PubMed]
8. Guan, J.; Li, J.; Yu, Y.; Mu, X.; Chen, A. DFT Studies of the Selective C–O Hydrogenolysis and Ring-Opening of Biomass-Derived Tetrahydrofurfuryl Alcohol over Rh(111) surfaces. *J. Phys. Chem. C* **2016**, *120*, 19124–19134. [CrossRef]
9. Feng, S.; Nagao, A.; Aihara, T.; Miura, H.; Shishido, T. Selective hydrogenolysis of tetrahydrofurfuryl alcohol on $Pt/WO_3/ZrO_2$ catalysts: Effect of WO_3 loading amount on activity. *Catal. Today* **2018**, *303*, 207–212. [CrossRef]

10. Tong, T.; Liu, X.; Guo, Y.; Norouzi Banis, M.; Hu, Y.; Wang, Y. The critical role of CeO_2 crystal-plane in controlling Pt chemical states on the hydrogenolysis of furfuryl alcohol to 1,2-pentanediol. *J. Catal.* **2018**, *365*, 420–428. [CrossRef]
11. Mizugaki, T.; Yamakawa, T.; Nagatsu, Y.; Maeno, Z.; Mitsudome, T.; Jitsukawa, K.; Kaneda, K. Direct Transformation of Furfural to 1,2-Pentanediol Using a Hydrotalcite-Supported Platinum Nanoparticle Catalyst. *ACS Sustain. Chem. Eng.* **2014**, *2*, 2243–2247. [CrossRef]
12. Wang, X.; Weng, Y.; Zhao, X.; Xue, X.; Meng, S.; Wang, Z.; Zhang, W.; Duan, P.; Sun, Q.; Zhang, Y. Selective Hydrogenolysis and Hydrogenation of Furfuryl Alcohol in the Aqueous Phase Using Ru–Mn-Based Catalysts. *Ind. Eng. Chem. Res.* **2020**, *59*, 17210–17217. [CrossRef]
13. Cao, Y.; Zhang, H.; Liu, K.; Zhang, Q.; Chen, K.-J. Biowaste-Derived Bimetallic Ru–MoOx Catalyst for the Direct Hydrogenation of Furfural to Tetrahydrofurfuryl Alcohol. *ACS Sustain. Chem. Eng.* **2019**, *7*, 12858–12866. [CrossRef]
14. Upare, P.P.; Kim, Y.; Oh, K.-R.; Han, S.J.; Kim, S.K.; Hong, D.-Y.; Lee, M.; Manjunathan, P.; Hwang, D.W.; Hwang, Y.K. A Bimetallic Ru3Sn7 Nanoalloy on ZnO Catalyst for Selective Conversion of Biomass-Derived Furfural into 1,2-Pentanediol. *ACS Sustain. Chem. Eng.* **2021**, *9*, 17242–17253. [CrossRef]
15. Koso, S.; Furikado, I.; Shimao, A.; Miyazawa, T.; Kunimori, K.; Tomishige, K. Chemoselective hydrogenolysis of tetrahydrofurfuryl alcohol to 1,5-pentanediol. *Chem. Commun. (Camb.)* **2009**, *15*, 2035–2037. [CrossRef]
16. Soghrati, E.; Kok Poh, C.; Du, Y.; Gao, F.; Kawi, S.; Borgna, A. C−O Hydrogenolysis of Tetrahydrofurfuryl Alcohol to 1,5-Pentanediol Over Bi-functional Nickel-Tungsten Catalysts. *ChemCatChem* **2018**, *10*, 4652–4664. [CrossRef]
17. Chen, L.; Ye, J.; Yang, Y.; Yin, P.; Feng, H.; Chen, C.; Zhang, X.; Wei, M.; Truhlar, D.G. Catalytic Conversion Furfuryl Alcohol to Tetrahydrofurfuryl Alcohol and 2-Methylfuran at Terrace, Step, and Corner Sites on Ni. *ACS Catal.* **2020**, *10*, 7240–7249. [CrossRef]
18. Zhu, Y.; Li, B.; Zhao, C. Cu nanoparticles supported on core–shell MgO-La_2O_3 catalyzed hydrogenolysis of furfuryl alcohol to pentanediol. *J. Catal.* **2022**, *410*, 42–53. [CrossRef]
19. Tan, J.; Su, Y.; Hai, X.; Huang, L.; Cui, J.; Zhu, Y.; Wang, Y.; Zhao, Y. Conversion of furfuryl alcohol to 1,5-pentanediol over CuCoAl nanocatalyst: The synergetic catalysis between Cu, CoOx and the basicity of metal oxides. *Mol. Catal.* **2022**, *526*, 112391. [CrossRef]
20. Dai, D.; Feng, C.; Wang, M.; Du, Q.; Liu, D.; Pan, Y.; Liu, Y. Ring-opening of furfuryl alcohol to pentanediol with extremely high selectivity over Cu/MFI catalysts with balanced Cu0–Cu+ and Brønsted acid sites. *Catal. Sci. Technol.* **2022**, *12*, 5879–5890. [CrossRef]
21. Liu, H.; Huang, Z.; Kang, H.; Xia, C.; Chen, J. Selective hydrogenolysis of biomass-derived furfuryl alcohol into 1,2- and 1,5-pentanediol over highly dispersed Cu-Al_2O_3 catalysts. *Chin. J. Catal.* **2016**, *37*, 700–710. [CrossRef]
22. Deng, Q.; Gao, R.; Li, X.; Wang, J.; Zeng, Z.; Zou, J.-J.; Deng, S. Hydrogenative Ring-Rearrangement of Biobased Furanic Aldehydes to Cyclopentanone Compounds over Pd/Pyrochlore by Introducing Oxygen Vacancies. *ACS Catal.* **2020**, *10*, 7355–7366. [CrossRef]
23. Lan, J.; Liu, P.; Fu, P.; Liu, X.; Xie, M.; Jiang, S.; Wen, H.; Zhou, Y.; Wang, J. Palladium confined in pure-silica TON zeolite for furfuryl alcohol hydrogenation into tetrahydrofurfuryl alcohol. *Microporous Mesoporous Mater.* **2021**, *322*, 111161. [CrossRef]
24. Zhu, Y.; Zhao, W.; Zhang, J.; An, Z.; Ma, X.; Zhang, Z.; Jiang, Y.; Zheng, L.; Shu, X.; Song, H.; et al. Selective Activation of C–OH, C–O–C, or C=C in Furfuryl Alcohol by Engineered Pt Sites Supported on Layered Double Oxides. *ACS Catal.* **2020**, *10*, 8032–8041. [CrossRef]
25. Kurniawan, R.G.; Karanwal, N.; Park, J.; Verma, D.; Kwak, S.K.; Kim, S.K.; Kim, J. Direct conversion of furfural to 1,5-pentanediol over a nickel–cobalt oxide–alumina trimetallic catalyst. *Appl. Catal. B Environ.* **2023**, *320*, 121971. [CrossRef]
26. Ma, R.; Wu, X.-P.; Tong, T.; Shao, Z.-J.; Wang, Y.; Liu, X.; Xia, Q.; Gong, X.-Q. The Critical Role of Water in the Ring Opening of Furfural Alcohol to 1,2-Pentanediol. *ACS Catal.* **2016**, *7*, 333–337. [CrossRef]
27. Zhang, J.; Li, C.; Chen, X.; Guan, W.; Liang, C. Insights into the reaction pathway of hydrodeoxygenation of dibenzofuran over MgO supported noble-metals catalysts. *Catal. Today* **2019**, *319*, 155–163. [CrossRef]
28. Zhang, W.; Xin, H.; Zhang, Y.; Jin, X.; Wu, P.; Xie, W.; Li, X. Bimetallic Pt-Fe catalysts supported on mesoporous TS-1 microspheres for the liquid-phase selective hydrogenation of cinnamaldehyde. *J. Catal.* **2021**, *395*, 375–386. [CrossRef]
29. Hronec, M.; Fulajtárova, K.; Soták, T. Highly selective rearrangement of furfuryl alcohol to cyclopentanone. *Appl. Catal. B Environ.* **2014**, *154–155*, 294–300. [CrossRef]
30. Shao, Y.; Wang, J.; Du, H.; Sun, K.; Zhang, Z.; Zhang, L.; Li, Q.; Zhang, S.; Liu, Q.; Hu, X. Importance of Magnesium in Cu-Based Catalysts for Selective Conversion of Biomass-Derived Furan Compounds to Diols. *ACS Sustain. Chem. Eng.* **2020**, *8*, 5217–5228. [CrossRef]
31. Martín, A.J.; Mitchell, S.; Mondelli, C.; Jaydev, S.; Pérez-Ramírez, J. Unifying views on catalyst deactivation. *Nat. Catal.* **2022**, *5*, 854–866. [CrossRef]
32. Lin, F.; Xu, M.; Ramasamy, K.K.; Li, Z.; Klinger, J.L.; Schaidle, J.A.; Wang, H. Catalyst Deactivation and Its Mitigation during Catalytic Conversions of Biomass. *ACS Catal.* **2022**, *12*, 13555–13599. [CrossRef]